Supplementary Information

The high-power conversion efficiency of two-dimensional GeSe/AsP van der Waals heterostructure for solar energy cells

Hong-Yao Liu, Chuan-Lu Yang*, Mei-Shan Wang, and Xiao-Guang Ma

School of Physics and Optoelectronic Engineering, Ludong University, Yantai 264025, the People's Republic of China

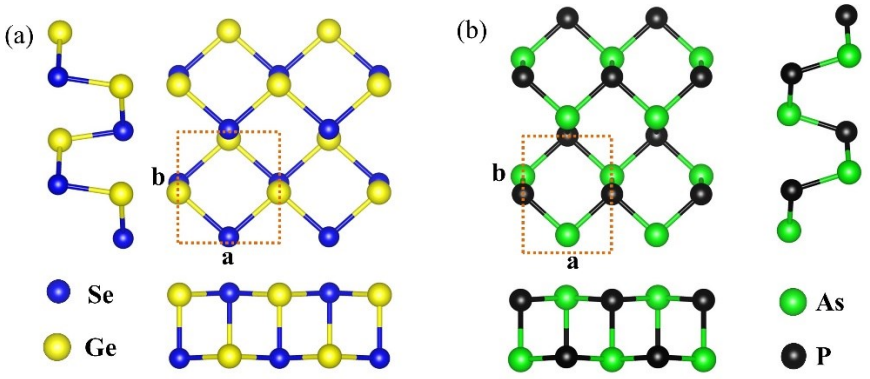

Fig. S1. The crystal structures of GeSe monolayer and AsP monolayer. ***a*** and ***b*** denote the lattice parameters. The blue, yellow, green, and black balls represent the Se, Ge, As, and P atoms, respectively.

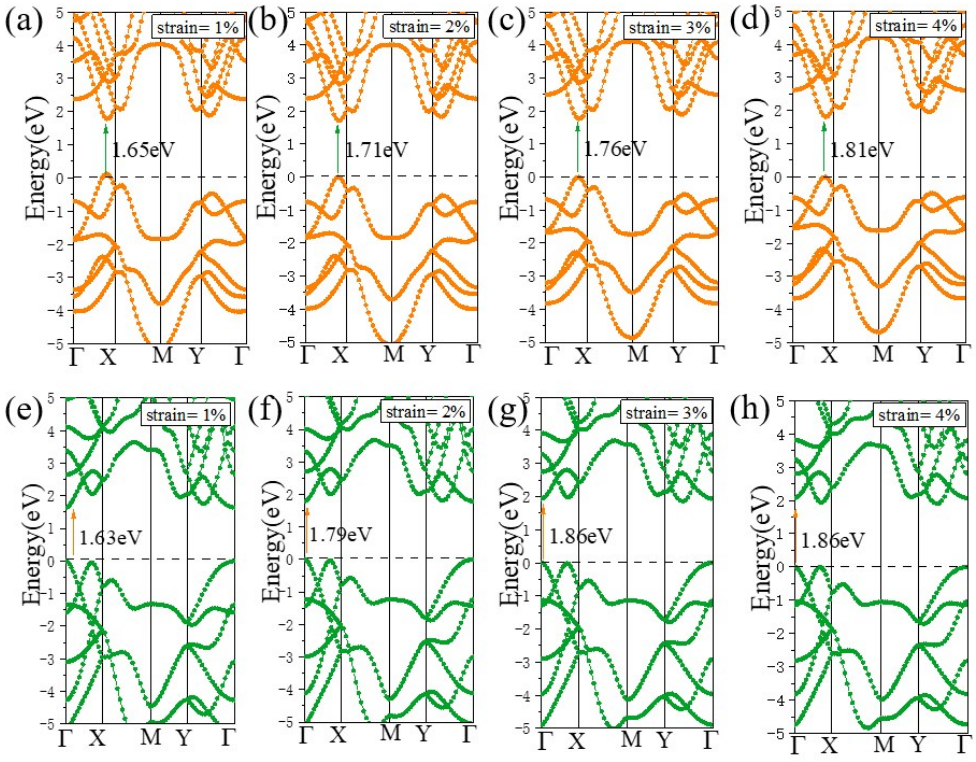

Fig. S2. The band structures of 2D GeSe (a)-(d) and 2D AsP (e)-(f) under 1% to 4% biaxial tensile strain.

*Corresponding author. Tel: +86 535 6672870. *E-mail address:* ycl@ldu.edu.cn. (C.L. Yang).

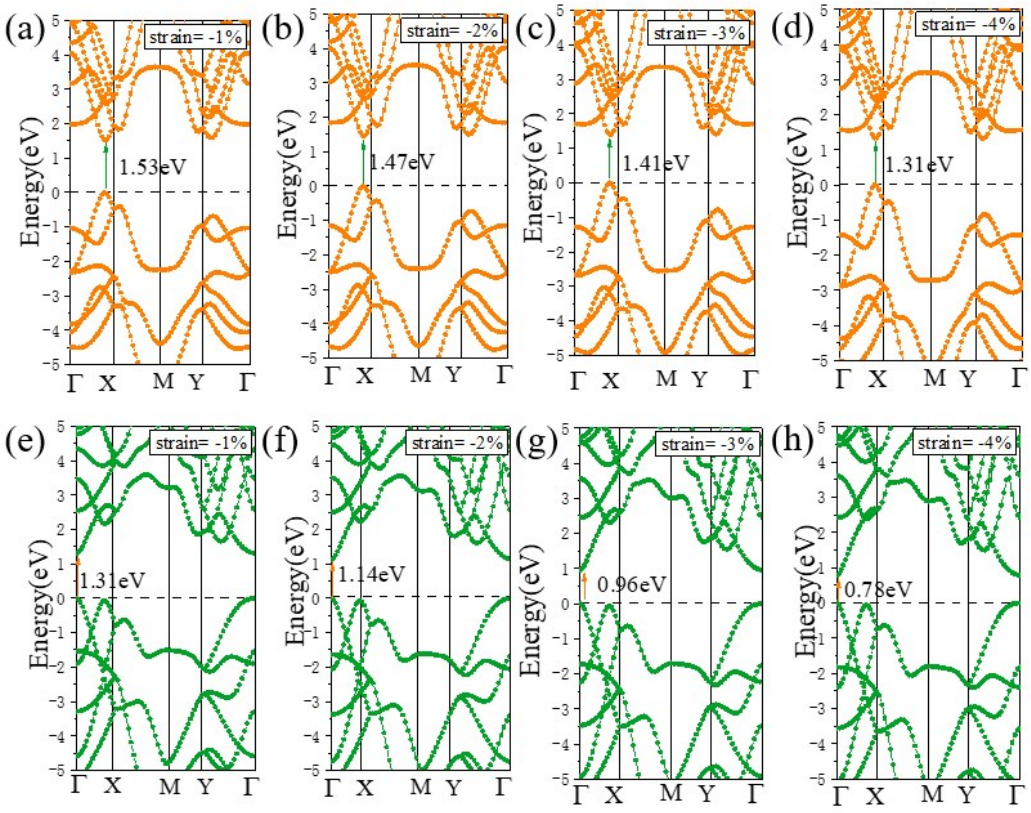

Fig. S3. The band structures of 2D GeSe (a)-(d) and 2D AsP (e)-(f) under 1% to 4% biaxial compressive strain.

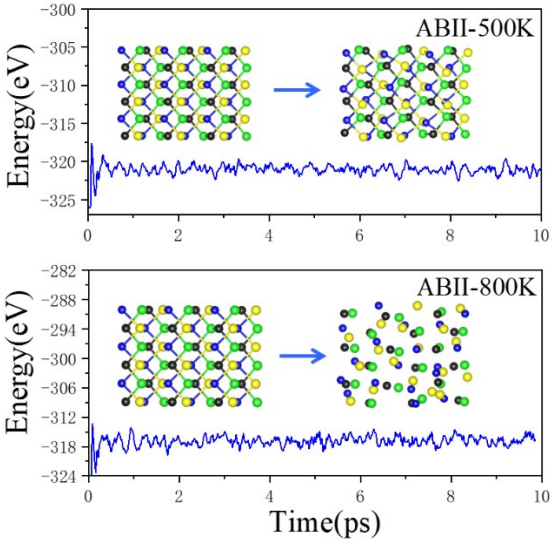

Fig. S4. Total energy fluctuations during the AIMD simulations at 500 and 800K for GeSe/AsP heterostructure with ABII-stacking.

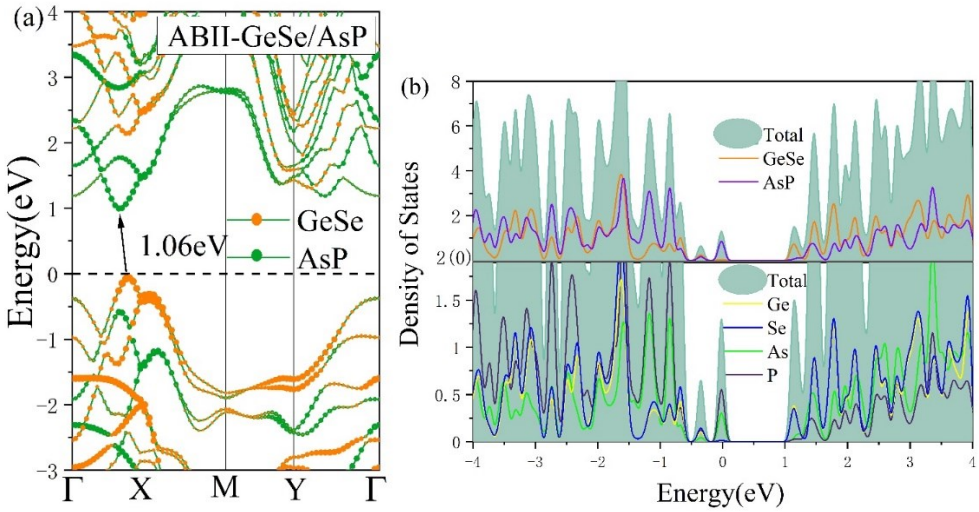

Fig. S5. The band structures (a) and projected densities of state (b) for GeSe/AsP heterostructure with ABII-stacking by HSE06 calculations, respectively.

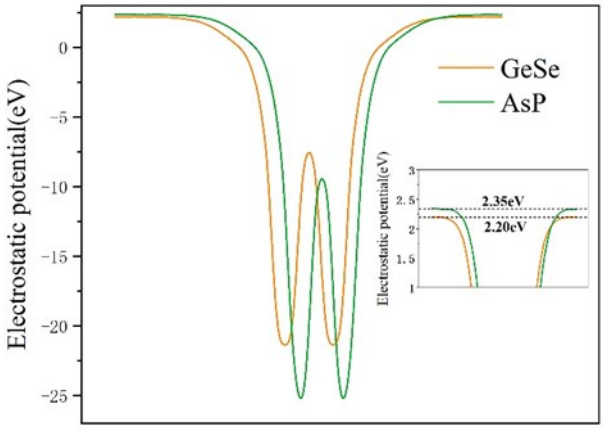

Fig. S6. The planar average potential of the independent GeSe and AsP monolayers.

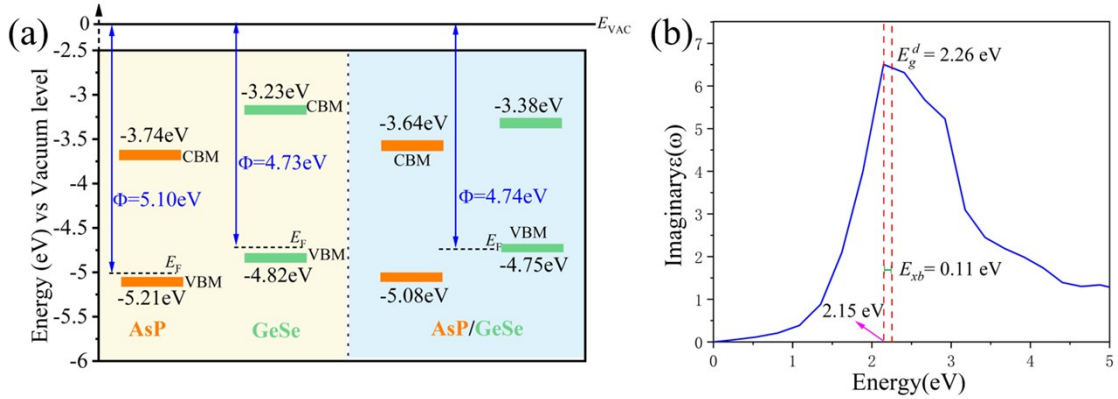

Fig. S7. (a) The band edge alignments, Fermi level, and work function of AsP, GeSe, and AsP/GeSe heterostructure, respectively. (b) The excitation binding energy and imaginary of dielectric function by GW+BSE.

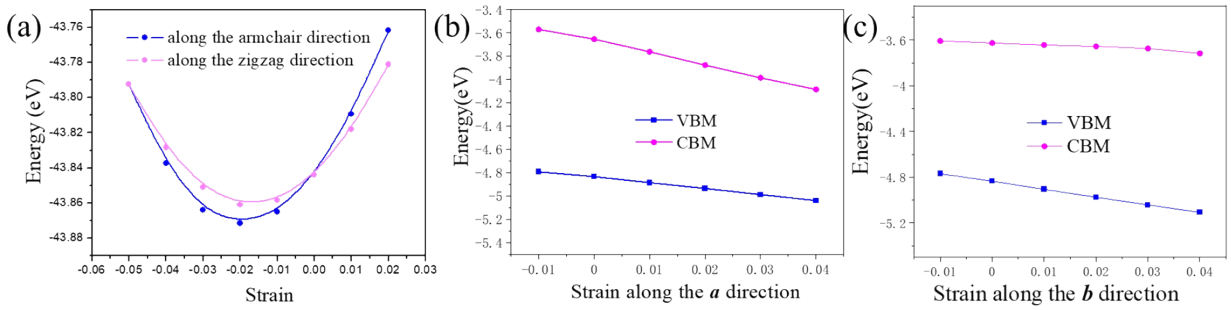

Fig. S8. The energy difference between the total energy of unstrained and strained GeSe/AsP heterostructure(a). Energy shift of CBM and VBM with respect to the lattice stretch and compression along with the armchair(b) and zigzag(c) directions of GeSe/AsP heterostructure.

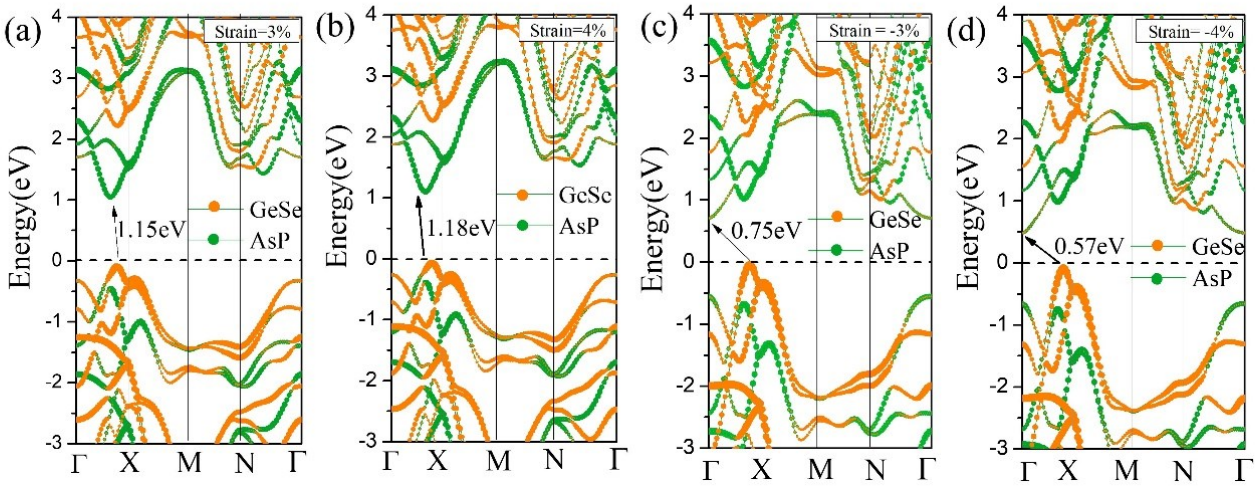

Fig. S9. The band structures of GeSe/AsP heterostructure under 3% and 4% biaxial strain.